Analysis of a Large Database of GCL-Geomembrane Interface Shear Strength Results

John S. McCartney, A.M.ASCE[1]; Jorge G. Zornberg, M.ASCE[2]; and Robert H. Swan Jr.[3]

Abstract: A database of 534 large-scale direct shear test results was assembled in this study to evaluate the interface shear strength between geosynthetic clay liners (GCLs) and geomembranes (GMs). The tests were conducted between 1992 and 2003 by a single independent laboratory using procedures consistent with current testing standards. The number of results in the database allowed quantification of the impact of GCL type, GM type, normal stress, and procedures for specimen hydration and consolidation on the shear strength of GCL-GM interfaces, as well as identification of sources of shear strength variability. The interface shear strength was found to be sensitive to the type of GCL internal reinforcement, GM polymer, and GM texturing, but not to the GM thickness or manufacturer. On average, the GCL internal shear strength was observed to be higher than the GCL-GM interface shear strength when tested using the same procedures. GCLs sheared internally show similar stress-displacement responses and friction angles to GCL-GM interfaces that incorporate a GCL with the same reinforcement type. Hydration under normal stresses below those used during shearing (followed by a consolidation period) led to higher GCL internal shear strength, but lower GCL-GM interface shear strength, than when hydration was conducted under the shearing normal stress. Such different responses are attributed to bentonite extrusion from the GCL into the interface. Good repeatability of test results was obtained using GCL and GM specimens from the same manufacturing lot, while high variability was obtained using specimens from different lots. GCL-GM interface peak shear strength variability was found to increase linearly with normal stress.

Introduction

Use of geomembranes (GMs) directly above a clay layer (i.e., a composite lining system) in hydraulic barrier systems such as landfill covers or bottom liners have been shown to perform better than single GMs or single compacted clay layers. Geosynthetic clay liners (GCLs) have often replaced the compacted clay layer in composite liners since they may offer equivalent or superior hydraulic performance while having limited thickness, good compliance with differential settlements of underlying soil or waste, easy installation, and low cost. GCLs are prefabricated geocomposite materials manufactured by bonding sodium bentonite clay to one or two geosynthetic backing materials (carrier geosynthetics). Stability is a major concern for side slopes in liners that include GCLs and GMs because of the very low shear strength of hydrated sodium bentonite, which has been reported to extrude

from the GCL leading to weakening of the interface (Triplett and Fox 2001). Accordingly, proper shear strength characterization is needed for the different liner materials and interfaces. In particular, a failure surface is likely to develop at the interface between a GCL and a GM. The shear strength of GCL-GM interfaces is the focus of the study presented herein.

Previous investigations have evaluated the GCL-GM interface shear strength using direct shear and ring shear tests (Gilbert et al. 1996, 1997; Hewitt et al. 1997; Triplett and Fox 2001). While these experimental studies have provided good insight into shear strength testing issues and variables affecting GCL-GM interface shear strength, available information on GCL-GM interface shear strength is still limited to specific ranges of normal stresses, GCL and GM types, and conditioning procedures. A GCL shear strength (GCLSS) database of results from 534 direct shear tests on the interface between different GCLs and GMs, conducted by a single laboratory, was assembled and evaluated in this study to identify and quantify the variables governing GCL-GM interface shear strength. Analysis of the results in the GCLSS database allows evaluation of: (i) the influence of different GCL and GM types on the GCL-GM interface shear strength; (ii) differences between GCL internal and GCL-GM interface shear strength; (iii) the effect of GCL conditioning on GCL-GM interface shear strength; and (iv) the variability in GCL-GM interface shear strength. This database also includes 414 direct shear tests conducted by the same laboratory used to quantify variables affecting the internal shear strength of GCLs, which were reported elsewhere (Zornberg et al. 2005). The results in the GCLSS database complement those presented in other databases (Chiu and Fox 2004) by providing more information specifically focused toward variables governing GCL-GM interface shear strength and inter-

[1]Barry Faculty Fellow and Assistant Professor, Univ. of Colorado at Boulder, Dept. of Civil, Environmental, and Architectural Engineering, 428 UCB, Boulder, CO 80309. E-mail: john.mccartney@colorado.edu

[2]Associate Professor, Univ. of Texas at Austin, 1 University Station C1792, Austin, TX 78712.

[3]Faculty Associate, Univ. of North Carolina at Charlotte Dept. of Engineering Technology, The William States Lee College of Engineering, 9201 University City Blvd, Smith 244 Charlotte, NC 28223-0001. E-mail: rswan1@uncc.edu

Table 1. Different GCLs in the Database

GCL product	GCL description	Product label[a]	GCL reinforcement label[b]	Upper carrier geotextile[c]	Lower carrier geotextile[c]
Bentomat (Arlington, IL) ST	Needle-punched, granular bentonite	A	np	W	NW
Claymax (Arlington, IL) 500SP	Stitch-bonded, granular bentonite	B	sb	W	W
Bentofix (Houston, TX) NS	Thermally locked, needle-punched, powdered bentonite	C	tl	W	NW
Bentofix NW	Thermally locked, needle-punched, powdered bentonite	D	tl	NW	NW
Bentofix NWL	GCL D with lower bentonite mass per unit area	E	tl	NW	NW
Claymax 200R	Unreinforced, granular bentonite	F	u	W	W
Bentomat DN	Needle-punched, granular bentonite	H	np	NW	NW

[a]Product label is consistent with Zomberg et al. (2005).
[b]np=needle punched, tl=thermally locked needle punched, sb=stitch bonded, u=unreinforced.
[c]W=woven carrier geotextile, NW=nonwoven carrier geotexile.

relationships between GCL internal and GCL-GM interface shear strength.

Database

Data Source

The large-scale direct shear tests in the GCLSS database were performed between 1992 and 2003 by the Soil-Geosynthetic Interaction laboratory, currently operated by SGI Testing Services (SGI). It should be noted that procedures used for all GCL direct shear tests conducted by SGI over the period 1992 to 2003 are consistent with ASTM D6243 and has been approved in 2008 (ASTM 2008), even though this standard was and originally between only and approved (and originally approved in 1998). Most tests in the GCLSS database were conducted for commercial purposes and, consequently, the test characteristics and scope were defined by project-specific requirements. Test conditions reported for each series in the GCLSS database include hydration time (t_h), consolidation time (t_c), normal stress during hydration (σ_h), normal stress during shearing (σ_n), and shear displacement rate (SDR).

Materials

Direct shear test results in the GCLSS database include 40 GCL-GM interfaces between eight GCL products (seven reinforced and one unreinforced) and seven GM types (from nine manufacturers). Table 1 summarizes the GCLs used in this study and provides a short description of the reinforcement characteris-

tics, bentonite characteristics (powdered or granular), and carrier geotextiles. The unreinforced GCL investigated in this study (GCL F) consists of an adhesive-bonded bentonite core attached to two woven polypropylene geotextiles. The stitch-bonded GCL investigated in this study (GCL B) consists of a bentonite layer stitched using synthetic yarns between two woven polypropylene carrier geotextiles. This GCL is no longer produced in the U.S. The needle-punched GCLs investigated in this study (GCLs A, G, and H) consist of a bentonite layer between two (woven or non-woven) carrier geotextiles, reinforced by pulling fibers through using a needling board. The fiber reinforcements are typically left entangled on the surface of the top carrier geotextile. Other needle-punched GCL products (GCLs C, D, and E) were thermal locked, which involves heating the GCL surface (Lake and Rowe 2000). For simplicity, thermal-locked needle-punched GCLs are referred to as thermal-locked GCLs in this paper. This study also evaluates the interface behavior of GCLs with either woven or nonwoven carrier geotextiles. A labeling system was developed to distinguish between the different GCL products, reinforcement alternatives, and the carrier geotextile under investigation in interface testing. The GCL product label is used as a prefix (e.g., A, B, C, D, E, F, or H), and a reinforcement label (e.g., u for unreinforced, np for needle punched, sb for stitch bonded, or tl for thermally locked needle punched) and a label for the carrier geotextile being sheared against the geomembrane to the right of a dash (e.g., NW or W) are included in parenthesis. For example, if the woven carrier geotextile side of GCL A were under investigation, it would be labeled as GCL A(npW), while if its nonwoven carrier geotextile side were under investigation, it would be labeled as GCL A(npNW).

Table 2. Different GMs in the Database

GM manufacturer	Manufacturing approach	Texturing approaches	GM manufacturer label	GM polymers evaluated from each manufacturer[a]
Oxychem (Dallas, TX)	Sheet calend.	Smooth	r	S/PVC
GSE (Houston, TX)	Blown film	Smooth and coextruded	s	T/HDPE, T/LLDPE, S/VLDPE
NSC (Galesburg, IL)	Blown film	Smooth and coextruded	t	T/HDPE, T/VLDPE, T/LLDPE, S/HDPE
Polyflex (Grand Prairie, TX)	Blown film	Smooth and coextruded	u	T/HDPE, T/VLDPE, T/LLDPE, S/VLDPE, S/LDPE, S/HDPE
Serrot (Huntington Beach, CA)	Blown film	Coextruded	v	T/HDPE
SLT (Woodlands, TX)	Die extrusion	Coextruded	w	T/HDPE
Watersaver (Denver, CO)	Sheet calend.	Smooth	x	S/PVC
EL (Tolleson, AZ)	Sheet calend.	Faille finish	y	T/PVC
EPI (Mancelona, MI)	Sheet calend.	Smooth	z	S/PVC

[a]Prefix "T" is for a textured surface, prefix "S" is for a smooth surface.

Table 2 summarizes the products from different GM manufacturers used in this study, and shows the GM polymer types and texture (textured or smooth surfaces) investigated in this study. Polyethylene (PE) is the most common polymer, as it is predominantly used in landfill applications. This study includes, in order of increasing flexibility, high density polyethylene (HDPE), linear low density polyethylene (LLDPE), and very-low density polyethylene (VLDPE) polymers. In addition, polyvinyl chloride (PVC) GMs, which are comparatively more flexible than PE GMs, were also evaluated in this study. The asperity heights of the textured GMs were not measured consistently in the database, as the tests were conducted for commercial purposes. Nonetheless, some studies (Triplett and Fox 2001; Ivy 2003; McCartney et al. 2005) indicate that asperity height can have an important influence on interface shear strength. A labeling system was also developed to distinguish between the GM manufacturers, textured and smooth surfaces, and polymer types. The manufacturing label is used as a prefix (e.g., r through z), while a texturing label (e.g., T for textured and S for smooth) and a polymer label are included in parenthesis. For example, if the textured side of an HDPE GM s was under investigation, it would be labeled as GM s(T/HDPE).

The direct shear equipment used in this study is similar to that reported by Zornberg et al. (2005). The bottom half of the shear box was filled with concrete sand, which provided a level surface for placement of the GM. The GM was secured with clamps to the bottom shear box. The GCL specimen was attached to a porous rigid substrate by wrapping extensions of the upper carrier geotextile (and occasionally lower carrier geotextile) around the rigid porous substrate, then placing another rigid porous substrate to provide a frictional connection. This assembly was placed in the upper half of the shear box. The rigid porous substrates have steel gripping teeth that allow shear stress transfer to the GCL by minimizing slippage between the carrier geotextiles and the substrates. Conditioning of specimens for GCL-GM shear strength testing involves hydration and (in some cases) subsequent consolidation of the bentonite core of the GCL while in contact with the GM. The specimen and rigid substrates were placed outside the direct shear device under the specified normal stress σ_h and soaked in tap water during the specified t_h. This assembly was then transferred to the direct shear device. The shearing normal stress (σ_n), which was often equal to σ_h, was subsequently applied. When σ_h was less than σ_n (i.e., to simulate field conditions representative of bottom liners), the normal stress was slowly ramped up from σ_h to σ_n, and pore pressures were allowed to dissipate during a consolidation period (t_c).

Shearing was conducted after GCL conditioning by applying a shear load to maintain a constant displacement rate. The maximum shear stress τ_p and the shear stress at large displacement τ_{ld} were defined for each test from the measured shear stress-displacement curve. The SDR used for most tests in the GCLSS database was 1.0 mm/min. While relatively fast for guaranteeing drained conditions as anticipated in the field, a SDR of 1.0 mm/min is typically used in engineering practice because of time and cost considerations (Triplett and Fox 2001; Fox and Stark 2004). Interface tests were also conducted using slower displacement rates (as low as 0.025 mm/min), but unlike GCL internal tests (Zornberg et al. 2005), the SDR showed little effect on the GCL-GM interface shear strength values. This is consistent with observations by Triplett and Fox (2001). Shearing was typically terminated when either a displacement of 75 mm or a constant τ_{ld} value was reached. In the tests reported in this database, failure was always observed along the GCL-GM interface. Although this test forced failure to occur along this interface, the GCL internal shear strength may be greater than the GCL-GM interface shear strength as shown by some results in the database. Testing was conducted under room temperature conditions, so shear strength values should be used carefully if extrapolated to high or low temperature environments.

Analysis of Results from Tests on Different GCL and GM Materials

This section summarizes the analyses conducted to evaluate the effect of GCL type, GM type, and testing procedures on GCL-GM interface shear strength. Specifically, these analyses provide: (i) comparison of the shear stress-displacement behavior of different interfaces; (ii) a simplified representation of GCL-GM interface shear strength suitable for comparison among different interfaces; and (iii) conventional representation of GCL-GM interface shear strength.

Shear Stress-Displacement Behavior

Typical shear stress-displacement curves for the interfaces between an 80-mil textured HDPE GM s and the woven carrier geotextiles of GCLs A (needle punched), and B (stitch bonded), and C (thermal locked) are shown in Figs. 1(a–c), respectively. The three interfaces shown in these figures were tested using the same σ_n (310.3 kPa), same t_h (168 hrs), same t_c (48 hrs), and same SDR (1.0 mm/min). For comparison, the figures also show internal shear stress-displacement curves for GCLs A, B, and C tested under the same conditions (Zornberg et al. 2005). Although the three interface direct shear tests involve the same combination of geosynthetics in contact (woven carrier geotextile of a GCL and a GM), the interface shear-displacement responses are significantly different. Indeed, the curves follow patterns similar to the corresponding internal shear-displacement curves. Specifically, the GCL A-GM interface shows a well defined peak (the highest τ_p) and a clear postpeak shear strength loss. This pattern is similar to that for GCL A when sheared internally, although it should be noted that the GCL A-GM internal τ_{ld} is lower than the GCL A-GM interface τ_{ld}. The GCL B-GM interface shows a rapid initial mobilization of shear strength until reaching a "yield" stress level, beyond which less pronounced hardening takes place until reaching τ_p. The displacement at peak for the GCL B-GM interface is larger than that observed for the GCL A-GM interface and only a little postpeak shear strength loss is observed for larger displacements. This observation may not be the same if GCL B were sheared in the cross-machine direction (opposite the direction of the stitches). In this case, the GCL B-GM interface also shows a similar shear displacement pattern as the GCL B internal curve. The GCL C-GM interface shows lower τ_p than the GCL A-GM interface, but both interfaces show a similar τ_{ld}. The GCL C internal shear-displacement curve also shows a similar response as the GCL C-GM interface curve. It should be noted that GCLs A and C are reinforced using similar needle-punching techniques and have the same specified peel strength [650 N/m obtained using ASTM D6496, (ASTM 2004)]. Consequently, the differences in behavior can be attributed to the effects of the thermal-locking process of GCL C. Although a similar pattern could have been expected among all interface shear-displacement curves (all interfaces involved a woven carrier geotextile and the same textured GM), the GCL-GM interface results show different patterns. However, the pattern of each GCL-GM interface shear displacement curve corresponds with that of the GCL sheared internally.
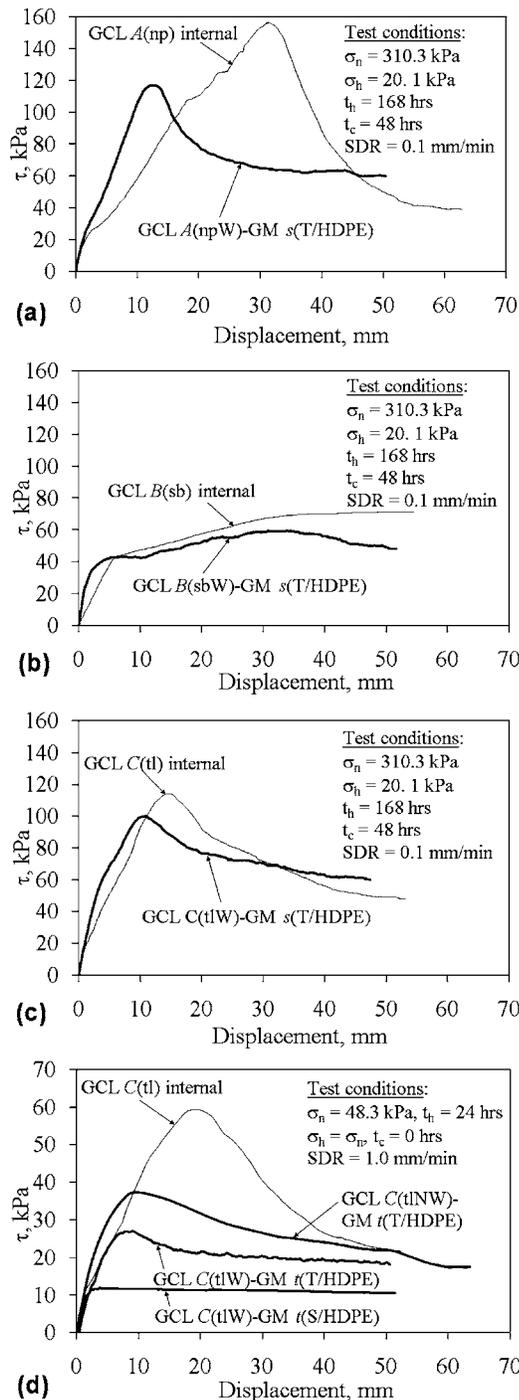
Fig. 1. Comparison between shear stress-displacement curves from GCL internal tests and GCL-GM interface tests involving: (a) woven side of GCL *A* (needle punched) with textured HDPE GM *s*, (b) woven side of GCL *B* (stitch bonded) with textured HDPE GM *s*; (c) woven side of GCL *C* (thermally locked) with textured HDPE GM *s*; and (d) nonwoven and woven sides of GCL *C* with textured and smooth HDPE GM *t*

As in the case of internal shear strength (Zornberg et al. 2005), the GCL fiber reinforcement influences the behavior of GCL-GM interfaces.

A comparison between the GCL internal and the GCL-GM interface shear stress-displacement curves is shown in Fig. 1(d) for tests conducted using the same GCL and different GM types.
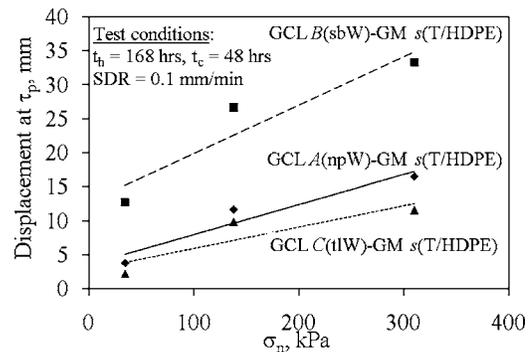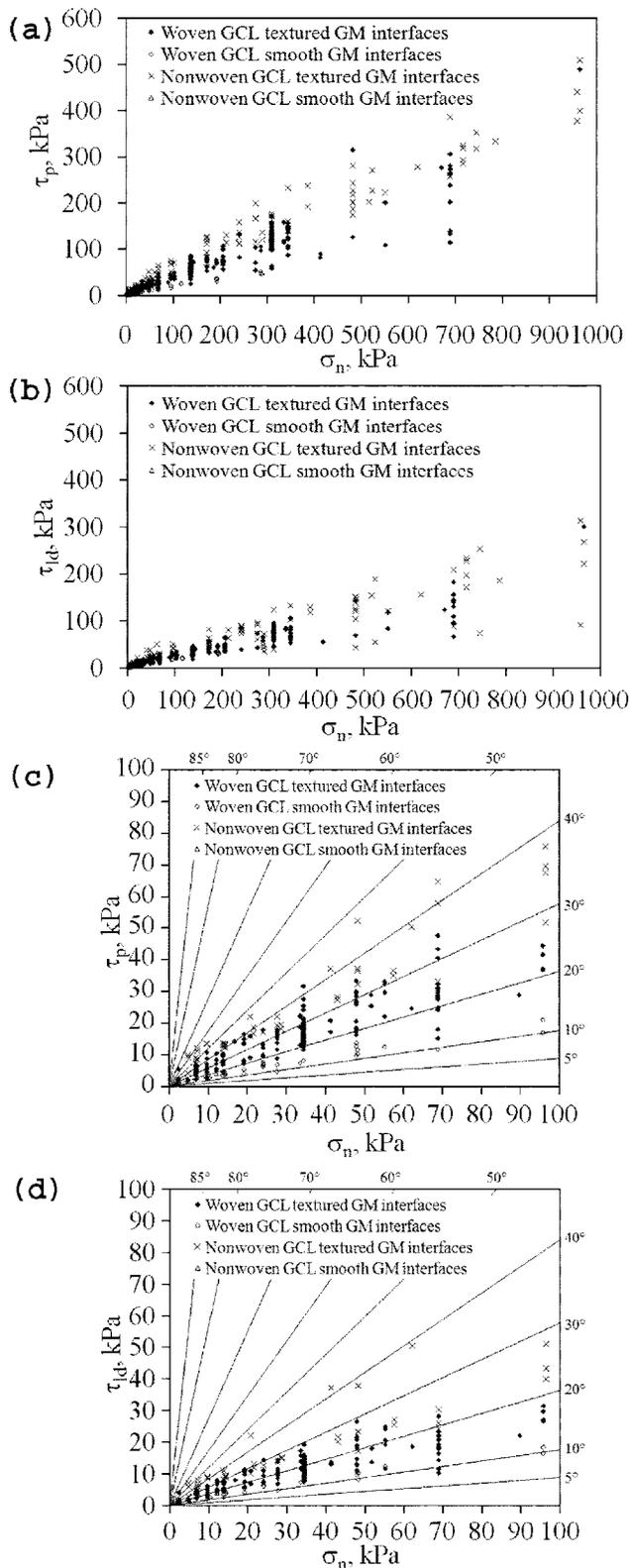

Fig. 2. Displacement at peak shear strength as a function of σ_n for interfaces between a textured HDPE GM and the woven sides of GCLs *A*, *B*, and *C*

The interface shear-displacement curves were obtained for both the woven and nonwoven sides of GCL *C* and HDPE GM *t* with textured and smooth finishes. The tests were conducted using the same σ_n (48.3 kPa), same t_h (24 hrs), same t_c (0 hrs), and same SDR (1.0 mm/min). Consistent with previous observations regarding the responses of interfaces between different GCLs and a textured GM [Fig. 1(a)], the GCL-GM interfaces in Fig. 1(d) show a similar pattern in the shear-displacement curves to that of the corresponding GCL internal test (although lower τ_p). The τ_p obtained using the woven side of the GCL is below that obtained using the nonwoven side of the GCL. The τ_p obtained using a smooth GM is significantly lower than the τ_p obtained using a textured GM. The curve obtained using a smooth GM showed a negligible postpeak shear strength loss (i.e., τ_p was similar to τ_{ld}).

The displacements at peak shear strength are shown in Fig. 2 for the interface shear tests shown in Figs. 1(a–c), along with the results from additional tests on these interfaces conducted using two other σ_n (34.5 and 137.9 kPa). The test results show increasing displacement at peak with increasing σ_n. Consistent with observations by Triplett and Fox (2001), GCL *B* shows much larger displacement at peak than the other GCL types, a characteristic that may be relevant for displacement-based stability analyses. The trends of the displacement at peak shear strength for the different GCLs are similar to those observed in internal shear tests on the same GCLs (Zornberg et al. 2005).

Overall GCL-GM Interface Shear Strength Assessment

The τ_p results for all GCL-GM interfaces in the GCLSS database are shown in Fig. 3(a). The wide range of normal stresses at which the interfaces were tested and the scatter in the data are apparent in this figure. The τ_{ld} data for all GCL-GM interfaces in the GCLSS database are shown in Fig. 3(b). Less scatter is observed in the τ_{ld} data than that observed in the τ_p data. As most data points shown in Figs. 3(a and b) correspond to comparatively low σ_n, Figs. 3(c and d) show a detail of the test results for σ_n values below 100 kPa. The results shown in Fig. 3(c) indicate that, unlike GCL internal shear strength results (Zornberg et al. 2005), the interface τ_p at low normal stress follows a trend approaching zero shear strength at zero normal stress. Consistent with findings of Triplett and Fox (2001), this indicates that cohesion intercept plays a less relevant role than in GCL internal shear strength. Only a slight nonlinearity is observed at low σ_n. Table 3 summarizes the shear strength parameters (c_p, ϕ_p, c_{ld}, ϕ_{ld}) for the 67 peak (τ_p) and large-displacement (τ_{ld}) failure envelopes (FEs).

Fig. 3. Shear strength results for all GCL-GM interfaces: (a) peak shear strength; (b) large-displacement shear strength; (c) peak shear strength (scaled); and (d) large-displacement shear strength (scaled)

The shear strength parameters were defined using linear regression of τ_p versus. σ_n, with the R^2 values in the regression exceeding 0.95.

The test results for all GCL-GM interfaces were grouped into 36 data sets defined according to the GM and GCL types as well as the GCL carrier geotextile type tested (woven or nonwoven). Table 4 summarizes the information about each data set, and provides the shear strength parameters for the peak and large-displacement envelopes (c_p, ϕ_p, c_{ld}, ϕ_{ld}). These GCL-GM interface data sets define preliminary shear strength values, as they do not account for the effect of GCL conditioning or GM asperity height. Comparison among the 36 GCL sets is aided by calculating the peak shear strength at a reference normal stress of 50 kPa (τ_{50}) using the GCL-GM interface data set envelopes. The τ_{50} peak shear strength is used to provide a single value with which to compare different data sets. A reference stress of 50 kPa is used to be consistent with that reported by Zornberg et al. (2005), who found that there were different trends in GCL internal shear strength under normal stresses above and below the swell pressure of GCLs. Although Zornberg et al. (2005) chose reference normal stresses of 50 and 300 kPa to bracket the approximate value of the swell pressure ($\sim$150 kPa), a single reference stress of 50 kPa is used in this study because the GCL-GM interface shear strength data can be well represented by a linear envelope. In order to quantify the variability of the shear strength for each GCL data set, the range of shear strength values was defined for this reference normal stress. Specifically, the lowest and highest shear strength values were defined using the individual failure envelopes (FE in Table 3) of each data set. Because of the small cohesion values of the interface shear strength envelopes, the general trends in the database can also be inferred from inspection of the ϕ values in Table 4. The following observations can be made regarding the peak shear strength of GCL-GM interfaces at a reference stress of 50 kPa:

- Consistent with the results of previous studies, woven GCL-textured GM interfaces generally have lower peak shear strength than nonwoven GCL-textured GM interfaces (Triplett and Fox 2001). The peak shear strength of all woven GCL-textured GM interfaces in the database (Set SS1) is characterized by c_p=5.9 kPa and ϕ_p=19.5° (τ_{50}=24 kPa), while the peak shear strength of all nonwoven GCL-textured GM interfaces in the database (Set SS2) is characterized by c_p =16.5 Kpa and ϕ_p=23.2° (τ_{50}=38 kPa). The peak shear strength involving textured GM interfaces show significant scatter [τ_{50} (Set SS1) ranges from 15 to 69 kPa and τ_{50} (Set SS2) ranges from 26 to 79 kPa].
- Woven GCL-smooth GM interfaces generally have lower peak shear strength than nonwoven GCL-smooth GM interfaces. The peak shear strength of all woven GCL-smooth GM interfaces in the database (Set SS3) is characterized by c_p =2.3 kPa and ϕ_p=9.3° (τ_{50}=10 kPa), while the peak shear strength of all nonwoven GCL-textured GM interfaces in the database (Set SS4) is characterized by c_p=0.4 kPa and ϕ_p =16.8° (τ_{50}=16 kPa). Less scatter is observed in the peak strength of interfaces involving smooth GMs than in those involving textured GMs [τ_{50} (Set SS3) ranges from 9 to 17 kPa; τ_{50} (Set SS4) ranges from 14 to 17 kPa].
- Comparison of the values for Sets SS1, SS2, SS3, and SS4 indicates that peak shear strength of interfaces involving textured GMs is higher than that of interfaces involving smooth GMs (for both woven and nonwoven GCLs), similar to observations by Triplett and Fox (2001). Further, based on results reported by Zornberg et al. (2005), the average peak GCL internal shear strength (τ_{50}=55 kPa) is higher than the average shear strength of the interface between GCLs and textured or smooth GMs. However, the GCL internal shear strength variability observed by Zornberg et al. (2005) is consistent with

Table 3. Summary of GCL-GM Interface Shear Envelopes in the Database

	Interface details				Text conditions					Peak			Large displacement		
Failure envelope	GCL tested	GM tested	GM thickness (mil)	Number of tests	SDR (mm/min)	t_h (hrs)	$\sigma_h^{\,a}$ (kPa)	t_c (hrs)	σ_s range (kPa)	c_p (kPa)	ϕ_p (°)	$s_p^{\,b}$ (kPa)	c_{ld} (kPa)	ϕ_{ld} (°)	$s_{ld}^{\,b}$ (kPa)
FE 1	A(npW)	s(T/HDPE)	80	3	1.0	0	0.0	0	241–965	45.5	25.3	49.8	6.6	16.8	11.6
FE 2	A(npW)	v(T/HDPE)	60 and 80	36	1.0	24	σ_n	0	6.9–689	5.8	20.7	15.9	6.7	11.0	9.0
FE 3	A(npW)	s(T/HDPE)	60 and 80	18	1.0	24	σ_n	0	6.9–483	4.1	21.4	15.2	3.5	11.9	12.9
FE 4	A(npW)	w(T/HDPE)	80	3	1.0	24	σ_n	0	38–345	22.4	20.2	10.4	14.0	9.1	3.9
FF.5	A(npW)	u(T/HDPE)	60	3	1.0	48	σ_n	0	51–103	8.3	18.2	28.7	3.1	16.7	10.8
FE 6	A(npW)	w(TMDPE)	80	3	1.0	48	4.8	0	89–276	11.8	12.8	41.6	12.8	6.4	44.5
FE 7	A(npW)	s(T/HDPE)	60	6	1.0	48	σ_n	0	51–345	16.4	12.2	41.6	6.7	8.4	17.6
FE 8	A(npW)	u(T/HDPE)	60	10	0.2	24	57.5	0	9.6–287	2.6	19.4	3.5	4.4	11.7	3.1
FE 9	A(npW)	s(T/HDPE)	60	3	0.1	48	σ_n	0	68–345	0.0	19.3	1.7	6.7	9.6	0.5
FE 10	A(npW)	t(T/HDPE)	60	3	1.0	72	6.9	24	172–690	23.8	9.4	3.3	23.1	3.8	4.9
FE 11	A(npW)	v(T/HDPE)	80	3	1.0	24	68.9	12	138–552	3.1	19.7	2.8	12.1	11.1	8.7
FE 12	A(npW)	s(T/HDPE)	80	162	0.1	168	20.7	48	34–310	6.0	20.5	10.5	5.2	12.7	6.0
FE 13	B(sbW)	s(T/HDPE)	60	6	1.0	0	0.0	0	12–48	1.6	23.3	3.4	2.0	17.7	3.3
FE 14	B(sbW)	t(T/HDPE)	60	5	1.0	0	0.0	0	2.4–48	1.3	31.2	0.9	1.7	22.5	1.1
FE 15	B(sbW)	t(T/HDPE)	40 and 60	18	1.0	24	13.8	0	2.4–103	3.9	17.9	3.2	4.1	9.8	2.8
FE 16	B(sbW)	s(T/HDPE)	60	9	1.0	24	σ_n	0	68–690	12.3	10.4	15.6	6.7	7.7	6.2
FE 17	B(sbW)	s(T/HDPE)	40 and 60	6	1.0	48	12.0	0	6.9–48	0.4	19.3	1.0	1.8	12.0	0.9
FE 18	B(sbW)	s(T/HDPE)	80	6	0.1	168	20.7	48	34–310	9.2	9.8	4.9	8.7	7.3	3.5
FE 19	C(tlW)	t(T/HDPE)	40	4	1.0	0	0.0	0	16–670	13.9	21.8	9.8	12.8	9.9	10.4
FE 20	C(tlW)	t(T/HDPE)	60	3	1.0	1	σ_n	0	20–62	1.2	20.9	0.3	1.1	15.8	0.3
FE 21	C(tlW)	t(T/HDPE)	60	3	1.0	24	13.8	0	34–138	0.0	23.3	0.7	1.0	16.2	1.3
FE 22	C(tlW)	t(T/HDPE)	60	10	0.2	24	57.5	0	9.6–335	7.9	18.3	4.6	4.9	13.1	3.3
FE 23	C(tlW)	t(T/HDPE)	60	3	0.025	24	13.8	0	34–138	0.0	22.6	1.5	0.0	18.2	0.7
FE 24	C(tlW)	s(T/HDPE)	80	6	0.1	168	20.7	48	34–310	3.7	17.9	3.8	3.3	10.4	3.7
FE 25	B(sbW)	u(T/VLDPE)	60	6	1.0	0	0.0	0	12–48	0.8	31.9	1.7	0.5	26.1	0.9
FE 26	B(sbW)	t(T/VLDPE)	60	5	1.0	24	4.8	0	2.4–48	2.5	30.3	0.4	1.7	23.5	0.8
FE 27	B(sbW)	u(T/VLDPE)	60	3	1.0	48	12.0	0	12–48	4.7	18.6	1.3	5.5	11.3	1.1
FE 28	A(npW)	u(T/VLDPE)	40	3	1.0	24	σ_n	0	2.4–19.2	4.1	33.2	0.2	2.6	24.2	0.2
FE 29	A(npW)	u(T/LLDPE)	40	4	1.0	72	σ_n	0	6.9–55.2	2.2	28.8	0.3	1.2	23.5	0.8
FE 30	A(npW)	t(T/LLDPE)	40	4	1.0	72	σ_n	0	6.9–55.2	2.5	26.3	0.5	1.6	19.3	0.8
FE 31	A(npW)	s(T/LLDPE)	40	3	1.0	72	0.0	48	4.8–19.2	0.2	20.6	0.8	0.6	15.8	0.1
FE 32	C(tlW)	u(T/LLDPE)	40	4	1.0	72	σ_n	0	6.9–55.2	2.2	29.3	0.5	2.4	21.9	0.6
FE 33	C(tlW)	t(T/LLDPE)	40	4	1.0	72	σ_n	0	6.9–55.2	0.1	27.9	0.2	1.1	18.3	0.4
FE 34	B(sbW)	t(S/HDPE)	60	5	1.0	24	4.8	0	2.4–48	0.5	11.1	0.2	0.5	11.1	0.2
FE 35	B(sbW)	u(S/HDPE)	60	10	0.2	24	57.5	0	9.6–287	3.9	9.2	0.5	2.9	9.2	0.5
FE 36	C(tlW)	t(S/HDPE)	60	3	1.0	48	10.3	0	10–69	0.9	8.8	2.1	0.9	8.8	2.1
FE 37	C(tlW)	t(S/HDPE)	60	10	0.2	24	55.2	0	9.7–290	3.6	8.6	2.6	2.4	8.0	2.1
FE 38	A(npW)	s(S/VLDPE)	40	2	1.0	24	4.8	0	14.4–23.9	0.2	14.0	0.0	0.2	14.0	0.0
FE 39	A(npW)	u(S/VLDPE)	40	3	1.0	24	σ_n	0	2.4–19.2	0.4	14.1	0.4	0.4	14.1	0.4
FE 40	A(npW)	u(S/VLDPE)	60	3	1.0	24	σ_n	0	13.8–34.5	0.6	13.1	N/A	0.0	13.1	N/A
FE 41	F(uW)	u(S/VLDPE)	40	3	1.0	168	σ_n	0	13.8–55.2	0.7	12.1	0.8	0.7	12.1	0.8
FE 42	A(npW)	y(T/PVC)	40	3	1.0	48	σ_n	0	4.8–24	0.2	18.5	0.6	0.2	18.5	0.6
FE 43	A(npW)	x(S/PVC)	30	3	1.0	24	4.8	0	13.8–41	1.7	16.7	0.2	1.7	16.7	0.2
FE 44	A(npW)	z(S/PVC)	40	3	0.05	24	0.0	48	2.4–36	0.6	15.9	0.1	0.6	15.9	0.1
FE 45	A(npNW)	s(T/HDPE)	80	3	1.0	0	0	0	241–965	44.8	25.7	4.4	3.1	15.1	10.1
FE 46	A(npNW)	w(T/HDPE)	80	3	1.0	0	0	0	69–276	18.5	33.0	3.7	7.4	16.7	5.6
FE 47	A(npNW)	t(T/HDPE)	80	3	1.0	24	σ_n	0	48–386	22.1	28.6	9.4	24.3	15.1	1.5
FE 48	A(npNW)	w(T/HDPE)	80	3	1.0	24	172	0	69–276	24.0	27.6	5.3	7.2	13.3	1.4
FE 49	A(npNW)	v(T/HDPE)	80	5	1.0	48	4.8	0	14–276	8.0	30.3	3.1	5.4	18.2	3.6
FE 50	A(npNW)	t(T/HDPE)	60	4	1.0	72	σ_n	0	69–517	7.4	20.8	1.9	1.9	16.3	4.9
FE 51	A(npNW)	v(T/HDPE)	80	3	1.0	24	345	14	621–965	61.4	19.2	2.5	34.3	11.0	0.9
FE 52	A(npNW)	v(T/HDPE)	80	3	1.0	24	68.9	12	138–552	11.7	20.8	1.1	3.1	12.0	2.4
FE 53	A(npNW)	v(T/HDPE)	60	3	1.0	24	0	24	4.8–23.9	1.1	33.8	0.1	0.4	27.1	0.1

Table 3. (*Continued.*)

	Interface details				Text conditions					Peak			Large displacement		
Failure envelope	GCL tested	GM tested	GM thickness (mil)	Number of tests	SDR (mm/min)	t_h (hrs)	$\sigma_h{}^a$ (kPa)	t_c (hrs)	σ_s range (kPa)	c_p (kPa)	ϕ_p (°)	$s_p{}^b$ (kPa)	c_{ld} (kPa)	ϕ_{ld} (°)	$s_{ld}{}^b$ (kPa)
FE 54	C(tlNW)	t(T/HDPE)	60	3	1.0	1	21	0	21–62	8.3	34.3	0.8	8.3	34.3	0.8
FE 55	C(tlNW)	t(T/HDPE)	40 and 80	9	1.0	24	σ_n	0	7.2–386	7.4	25.9	3.4	4.6	16.2	1.6
FE 56	C(tlNW)	v(T/HDPE)	60	3	1.0	24	σ_n	0	6.9–35	3.0	32.2	0.2	2.2	20.8	0.2
FE 57	D(tlNW)	v(T/HDPE)	80	5	1.0	24	σ_n	0	97–958	53.7	19.0	14.0	34.0	3.0	10.9
FE 58	D(tlNW)	t(T/HDPE)	60	6	1.0	24	0.0	24	97–482	33.5	17.2	10.7	32.3	4.7	25.2
FE 59	D(tlNW)	t(T/HDPE)	80	6	1.0	24	69	24	6.9–690	14.1	20.3	14.4	13.1	6.9	11.8
FE 60	E(tlNW)	t(T/HDPE)	40	8	1.0	336	σ_n	0	14–58	4.2	28.6	1.0	3.6	21.7	0.7
FE 61	H(tlNW)	x(T/HDPE)	60 and 80	20	1.0	24	σ_n	0	48–958	22.1	22.6	18.4	12.4	16.2	19.2
FE 62	H(tlNW)	t(T/HDPE)	80	3	1.0	24	3.4	24	172–690	4.8	32.2	0.4	43.8	24.9	72.8
FE 63	H(tlNW)	s(T/HDPE)	80	3	1.0	24	3.4	24	6.9–28	48.6	26.3	17.1	43.8	13.6	6.4
FE 64	H(tlNW)	s(T/HDPE)	40	6	0.25	96	0	24	4.8–9.6	5.7	39.4	0.4	4.4	24.5	0.5
FE 65	H(tlNW)	z(S/PVC)	40	2	1	24	4.8	0	14–24	0.3	18.0	N/A	0.1	17.8	N/A
FE 66	H(tlNW)	r(S/PVC)	40	3	1	24	σ_n	0	4.8–24	0.8	15.1	0.0	0.8	15.1	0.1

[a] $\sigma_h = \sigma_a$ means that the hydration stress used for each specimen equals the normals tress to be used during shearing.

[b] s_p and s_{kl} = standard deviationsof the lienar regressions for the peak and large displacement shear strength data, respectively.

that of GCL-textured GM interfaces (τ_{50} ranging from 13 to 71 kPa), and it is possible that the GCL internal shear strength may be lower than the GCL-GM interface shear strength.

- Comparison of Sets SS5–SS12 in Table 4 indicates that interfaces involving flexible GMs lead to higher shear strength than those involving rigid GMs. Specifically, interfaces involving the relatively flexible VLDPE GMs (Set SS5, τ_{50}=29 kPa) show higher strength than interfaces involving the relatively rigid HDPE GMs (Set SS7, τ_{50}=24 kPa. The interfaces involving textured LLDPE GMs (Set SS6, τ_{50}=28 kPa) show intermediate strength values while the faille-finish PVC GMs (Set SS8, τ_{50}=17 kPa) show the lowest shear strength due to their smaller asperity height. Although the textured HDPE GM interfaces in this comparison were tested over a much wider range of normal stresses, investigations considering only those tests conducted at normal stresses less than 50 kPa led to similar conclusions. Nonetheless, these conclusions should only be considered for low normal stress applications. Among the tests involving smooth GMs, interfaces with flexible PVC GMs (Set SS12) have the highest strength (τ_{50}=16 kPa), while interfaces involving the more rigid smooth HDPE GMs (Set SS11) have the lowest strength (τ_{50}=11 kPa).

- The effect of GCL reinforcement types is evaluated by comparing the results of Sets SS13–SS15 for woven GCL interfaces and the results of Sets SS24–SS28 for nonwoven GCL interfaces. The peak shear strength of the interfaces involving woven needle-punched GCL *A* (Set SS13, τ_{50}=23 kPa) is similar to that of interfaces involving woven thermal-locked GCL *C* (Set SS15, τ_{50}=21 kPa) but higher than that of interfaces involving woven stitch-bonded GCL *B* (Set SS14, τ_{50}=17 kPa). This trend is consistent with that observed for the internal shear strength of the same GCLs (Zornberg et al. 2005). The peak shear strength of interfaces involving nonwoven GCLs (Sets SS24–SS28) is consistently higher than that of interfaces involving woven GCLs.

- For the textured HDPE GMs tested, the interface shear strength results are reasonably independent of the GM manufacturer. This can be evaluated by comparing the results of

Sets SS16–SS20 for woven GCL interfaces and of Sets SS29–SS32 for nonwoven GCL interfaces. The interfaces involving a woven GCL and textured HDPE GMs from multiple manufacturers have similar shear strength ($\tau_{50} \approx 23$ kPa). It should be noted that the GMs evaluated in this study were all blown-film geomembranes with texturing consisting of coextruded asperities, so this observation should not be extrapolated to interfaces involving GMs that use structured or calendared texturing. The interfaces involving nonwoven GCL and textured HDPE GMs from multiple manufacturers have similar strength ($\tau_{50} \approx 36$ kPa). Although it appears that the nonwoven interfaces with GM manufacturer *w* were higher, it should be noted that this interface was sheared under unhydrated conditions (FE 46), a feature not captured by this analysis.

- Interface shear strength results are independent of GM thickness. This can be evaluated by comparing Sets SS21–SS23 for woven GCL interfaces and Sets SS34–SS36 for nonwoven GCL interfaces (thicknesses of 40, 60, and 80 mil). Sets SS21–SS23 show a similar τ_{50} of 23 kPa while Sets SS34–SS36 have a similar τ_{50} of 31 kPa.

In summary, the results in Table 4 indicate that the peak shear strength values of the GCL-GM interfaces are sensitive to the type of GCL carrier geotextile, the flexibility of different GM polymer types, and the GCL reinforcement type. However, the peak shear strength was not sensitive to the GM manufacturer or GM thickness.

Inspection of ϕ_{ld} values shown in Table 4 leads to the following observations regarding the large-displacement shear strength of GCL-GM interfaces:

- The large-displacement friction angles of woven and nonwoven GCL-textured GM interfaces [ϕ_{ld} (Set SS1)=11.3° and ϕ_{ld} (Set SS2)=13.0°] are lower than the corresponding peak friction angles, indicating substantial postpeak shear strength loss. Instead, the large-displacement friction angles of woven and nonwoven GCL-smooth GM interfaces [ϕ_{ld} (Set SS3) =8.8° and ϕ_{ld} (Set SS4)=16.9°] are similar to the corresponding peak friction angles indicating little postpeak shear strength loss for interfaces involving smooth GMs. The ϕ_{ld} for the smooth GM interfaces in Set SS4 is higher than that in the

Table 4. GCL-GM Interface Data Sets for Overall Shear Strength Assessment

GCL-GM data set	Set description[a]			Peak			Large displacement	
	GCL grouping	—	GM grouping	c_p (kPa)	ϕ_p (°)	τ_{50} [Range][b] (kPa)	c_{ld} (kPa)	ϕ_{ld} (°)
SS1	Woven (W)	—	Textured (T)	5.9	19.5	24 [15 (FE 44) to 69 (FE 1)]	6.0	11.3
SS2	Nonwoven (NW)	—	T	16.5	23.2	38 [26 (FE 50) to 79 (FE 51)]	12.2	13.0
SS3	W	—	Smooth (S)	2.3	9.3	10 [9(FE 36) to 17 (FE 42)]	2.1	8.8
SS4	NW	—	S	0.4	16.8	16 [14 (FE 66) to 17 (FE 65)]	0.3	16.9
SS5	W	—	T/VLDPE	3.4	27.4	29 [21 (FE 27) to 37 (FE 28)]	2.4	21.7
SS6	W	—	T/LLDPE	0.8	28.8	28 [19 (FE 32) to 30 (FE 33)]	1.0	21.3
SS7	W	—	T/HDPE	5.9	19.4	24 [18 (FE 9) to 69 (FE 1)]	6.0	11.3
SS8	W	—	T/PVC	1.6	16.7	17 [17 (FE 43) to 17 (FE 43)]	1.6	16.7
SS9	W	—	S/VLDPE	0.4	14.1	13 [13 (FE 38) to 13 (FE 39)]	0.4	14.1
SS10	W	—	S/LLDPE	0.9	12.1	12 [11 (FE 41) to 11 (FE 40)]	0.3	12.5
SS11	W	—	S/HDPE	2.5	9.2	11 [9 (FE 36) to 11 (FE 35)]	2.0	8.8
SS12	W	—	S/PVC	0.8	16.4	16 [15 (FE 44) to 17 (FE 43)]	0.8	16.4
SS13	A(npW)	—	T/HDPE	4.4	20.9	23 [19 (FE 9) to 69 (FE 1)]	5.8	11.8
SS14	B(sbW)	—	T/HDPE	6.6	12.1	17 [18 (FE 18) to 23 (FE 13)]	4.6	9.2
SS15	C(tlW)	—	T/HDPE	2.0	21.0	21 [20 (FE 24) to 34 (FE 19)]	7.4	11.0
SS16	W	—	s(T/HDPE)	4.4	20.1	23 [18 (FE 9) to 69 (FE 1)]	4.0	12.2
SS17	W	—	t(T/HDPE)	9.2	15.6	23 [20 (FE 15) to 34 (FE 19)]	7.6	9.6
SS18	W	—	u(T/HDPE)	3.7	19.3	21 [20 (FE 8) to 25 (FE 5)]	5.6	12.2
SS19	W	—	v(T/HDPE)	5.5	20.6	24 [21 (FE 11) to 25 (FE 2)]	7.0	11.1
SS20	W	—	w(T/HDPE)	6.6	19.5	24 [23 (FE 6) to 41 (FE 4)]	5.4	11.2
SS21	W	—	T/HDPE 40-mil	2.3	22.8	23 [18 (FE 17) to 34 (FE 19)]	4.5	10.7
SS22	W	—	T/HDPE 60-mil	6.0	17.9	22 [18 (FE 9) to 32 (FE 14)]	7.3	10.0
SS23	W	—	T/HDPE 80-mil	3.9	21.0	23 [18 (FE 18) to 69 (FE 1)]	2.9	13.0
SS24	A(npNW)	—	T/HDPE	23.7	23.5	45 [31 (FE 52) to 79 (FE 51)]	12.1	13.5
SS25	C(tlNW)	—	T/HDPE	9.0	25.8	33 [32 (FE 55) to 42 (FE 54)]	8.8	15.9
SS26	D(tlNW)	—	T/HDPE	21.4	20.5	40 [33 (FE 59) to 71 (FE 57)]	25.7	4.5
SS27	E(tlNW)	—	T/HDPE	4.2	28.6	31 [31 (FE 60) to 31 (FE 60)]	3.6	21.7
SS28	H(npNW)	—	T/HDPE	15.7	23.8	38 [36 (FE 62) to 73 (FE 63)]	9.4	16.5
SS29	NW	—	s(T/HDPE)	14.3	23.6	36 [43 (FE 61) to 73 (FE 63)]	11.3	15.2
SS30	NW	—	t(T/HDPE)	12.7	23.5	34 [31 (FE 60) to 49 (FE 47)]	14.1	11.8
SS31	NW	—	v(T/HDPE)	18.1	21.6	38 [31 (FE 52) to 79 (FE 51)]	20.0	5.6
SS32	NW	—	w(T/HDPE)	21.3	30.4	51 [50 (FE 48) to 51 (FE 46)]	7.3	15.0
SS34	NW	—	T/HDPE 40-mil	7.0	25.8	31 [31 (FE 60) to 47 (FE 64)]	4.4	20.8
SS35	NW	—	T/HDPE 60-mil	12.0	21.9	32 [26 (FE 50) to 49 (FE 58)]	9.4	14.5
SS36	NW	—	T/HDPE 80-mil	10.0	23.2	31 [31 (FE 52) to 79 (FE 51)]	15.6	12.2

[a]Sets do not capture the effect of specimen conditioning and SDR and should not be used for design.

[b]Range defined by the lowest τ_p (and corresponding FE) and the highest τ_p (and corresponding FE), defined at a reference stress of $\sigma_n = 50$ kPa using the shear strength parameters from Table 4.

other interface sets due to the low normal stresses under which the tests in this set were performed.
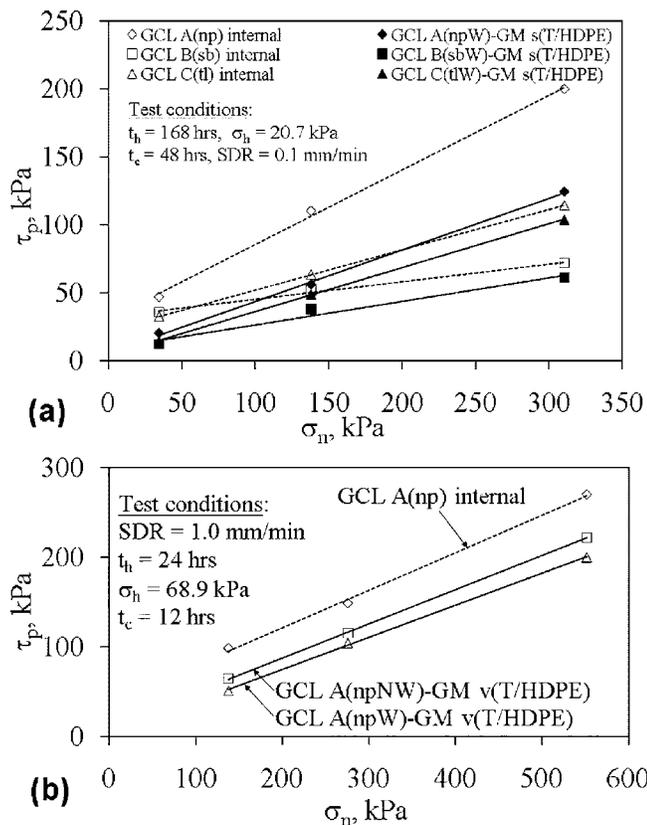
- The range of large-displacement shear strength for the GCL-GM interface data sets in Table 4 (ϕ_{ld} ranging from 4.5–21.7°), as well as that presented for the individual failure envelopes in Table 3 (ϕ_{ld} ranging from 3.0–34.3°), indicates that the variability in large-displacement shear strength is not-negligible. This is consistent with observations made from large-displacement GCL internal shear strength (Zornberg et al. 2005).

Assessment of Shear Strength of GCL-GM Interfaces Tested under Similar Conditioning Procedures

Shear strength characterization for design purposes requires an accurate representation of shear strength envelopes and assess- ment of the effect of GCL conditioning. Some comparisons be- tween the shear strength of GCL-GM interfaces prepared using similar conditioning procedures are discussed below.

The GCL-GM interface peak failure envelopes obtained for different GCL types (FE 12 for GCL A, FE 18 for GCL B, FE 24 for GCL C) and the same GM s tested under the same conditions ($t_h = 168$ hrs, $t_c = 48$ hrs, SDR = 0.1 mm/min) are shown in Fig. 4(a). The shear stress-displacement curves of the tests conducted under $\sigma_n = 310.3$ kPa are shown in Fig. 1. Fig. 4(a) also shows the GCL internal failure envelopes obtained using the same GCL con- ditions (Zornberg et al. 2005). The results in Fig. 4(a) indicate that interfaces including GCL A, C, and B show the highest, in- termediate, and lowest τ_p, respectively. This is the same trend shown by the internal peak shear strength of GCLs A, B, and C. The internal peak shear strength envelope of each GCL is consis-

Fig. 4. Shear strength envelopes for same conditioning procedures: (a) peak shear strength values for different GCLs sheared internally and along the interface between the woven geotextile of the GCL and a textured HDPE GM; (b) peak shear strength values for GCL *A* sheared internally and along the interface between the woven and nonwoven geotextiles of the GCL and a textured HDPE GM
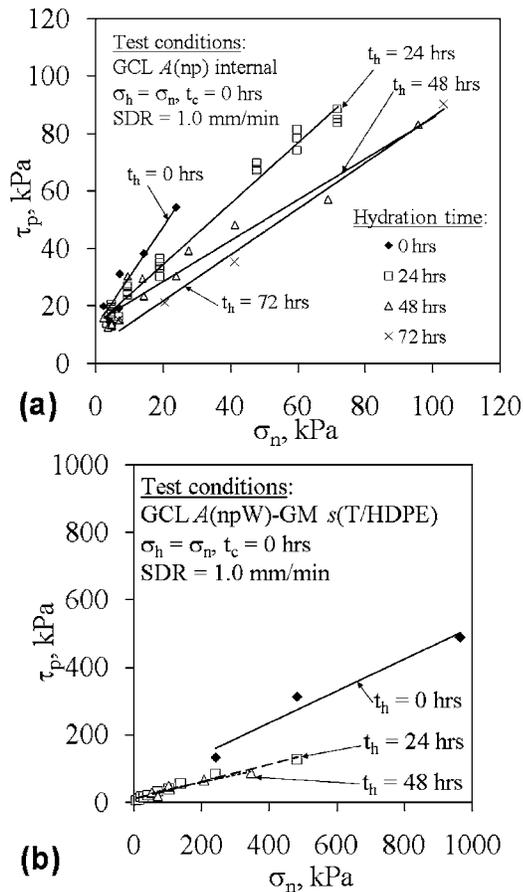
fibers from the thermal-locking process. It is possible that the textured asperities of the GM may interact in different ways with the entangled fibers on GCL *A* (i.e., the "Velcro effect") than the smoother surfaces of GCLs *B* and *C* (McCartney et al. 2005). This may be evidenced by the greater postpeak drop in shear stress observed in GCL *A* interface tests than in the other GCL interfaces. Nonetheless, it is also likely that different amounts of bentonite were extruded from the three GCLs into the GCL-GM interface during hydration. Posttest observations of the interfaces after shearing indicates that hydration and subsequent shearing of the GCL-GM interface led to extrusion of bentonite from the GCL into the GCL-GM interface, consistent with observations by Triplett and Fox (2001). Although quantitative measurements of the volume of bentonite extrusion were not made for the tests shown in Fig. 4(a), visual observations from free swell tests indicate that the different reinforcement approaches led to different resistances to swelling. Specifically, the relatively rigid stitches in GCL *B* provided the most resistance to swelling (at least in the vicinity of the stitches), the thermal-locking of GCL *C* was found to provide a relatively uniform, rigid connection between the reinforcing fibers and the woven carrier geotextile, while the loose fiber reinforcements of GCL *A* were found to provide the least resistance to swelling [consistent with observations by Lake and Rowe (2000)]. A higher tendency of the bentonite to extrude through the woven carrier geotextiles is expected in cases where the reinforcement connections are rigid (i.e., more resistant to swelling). Additional research is needed on the quantification of bentonite extrusion from GCLs.

Dry migration of bentonite through the carrier geotextiles of the GCL during shipping and handling also plays a role in GCL-GM interface shear strength. The amount of dry bentonite on the surfaces of the GCL is difficult to quantify and depends on different variables. Nonetheless, greater amounts of dry bentonite were visible on the surface of GCLs with woven carrier geotextiles than on those with nonwoven carrier geotextiles. Further, greater amounts of dry migration were observed for GCLs with powdered bentonite (GCLs) *C*, *D*, *E* than for GCLs with granular bentonite (GCLs *A*, *B*, *F*, *H*, *G*).

The internal peak envelope for GCL *A*, as well as the interface peak envelopes for interfaces involving the textured HDPE GM *v* and the woven and nonwoven sides of GCL *A* (FE 11 and 52 in Table 3), are shown in Fig. 4(b). Consistent with the results shown in Fig. 4(a), the peak shear strength envelopes in Fig. 4(b) show a similar slope (i.e., similar friction angle). Although lower than the internal GCL shear strength, the nonwoven GCL-GM interface shear strength is slightly higher than that of the woven GCL-GM interface. The internal GCL large-displacement envelopes are similar in trend and magnitude to the woven and nonwoven GCL-GM interface large-displacement envelopes (see FE 11 and 52 in Table 3).

Effect of Conditioning on Interface Shear Strength

Conditioning of GCL specimens involves hydration of the bentonite component, which usually has an initial gravimetric water content of approximately 10%. Hydration of the bentonite leads to an increase in volume (swelling) that depends on the applied normal stress. As hydration of the GCL in the field occasionally occurs under normal stresses below the final expected values, specimen conditioning also includes subsequent consolidation under the normal stress to be used during shearing. Results from GCL internal and GCL-GM interface direct shear tests using dif-

tently higher than (and approximately parallel to) the corresponding GCL-GM interface shear strength. That is, internal and interface shear strength envelopes involving the same GCLs had similar friction angles. Since the internal shear strength is consistently higher than the interface shear strength, the stability of a GCL-GM composite liner is expected to be governed by the interface shear strength properties if design is based on peak strength. Unlike the peak failure envelopes, the GCL internal and GCL-GM interface large-displacement failure envelopes were found to be similar in both trend and magnitude (see FE 12, 18, and 24 in Table 3). Consequently, the stability of a GCL-GM composite liner could be governed by either the internal or interface shear strength properties if design is based on large-displacement conditions.

As the test conditions and geomembrane were the same in each of the three interfaces whose strengths are shown in Fig. 4(a), the differences in the shear strength results for these three interfaces can be attributed to the characteristics of the GCL. Specifically, the primary differences between the woven carrier geotextile side of GCLs *A*, *B*, and *C* are the surface roughness and the tendency for different amounts of bentonite extrusion during hydration and shearing. With respect to the surfaces of the three GCLs, GCL *A* has fibers from the needle-punching process entangled on the woven carrier geotextile of the GCL, the woven carrier geotextile of GCL *B* is relatively smooth due to the continuous stitched reinforcements, and the woven carrier geotextile of GCL *C* has a burnished surface with small balls of melted

Fig. 5. Effect of hydration under $\sigma_h=\sigma_n$ on: (a) internal GCL peak shear strength; (b) woven GCL-GM interface peak shear strength

Fig. 6. Effect of hydration under $\sigma_h<\sigma_n$ with $t_c=0$ hrs on: (a) internal GCL peak shear strength; (b) woven GCL-GM interface peak shear strength

ferent conditioning procedures were used to evaluate the effects of hydration and consolidation on the GCL internal and GCL-GM interface peak shear strength. This evaluation extends the discussion of McCartney et al. (2004a), although the trends in the datasets have been reinterpreted. The effect of conditioning on large-displacement shear strength (from GCL internal and GCL-GM interface tests) was also investigated. However, large-displacement envelopes were found to be insensitive to conditioning procedures, so they are not discussed in this section.

The effect of t_h on the peak internal shear strength of GCL A (needle punched) tested using σ_n ranging from 2.4 to 100 kPa is shown in Fig. 5(a). The specimens were conditioned using the same normal stress during hydration and shearing (i.e., $\sigma_h=\sigma_n$). The results show a decreasing τ_p with increasing t_h. However, no further changes in τ_p are observed for t_h beyond 48 hrs. The results in Fig. 5(b) for woven GCL-GM interfaces (needle-punched GCL A and a textured HDPE geomembrane s) indicate that hydration time has a similar effect on the GCL-GM interface τ_p as on the GCL internal τ_p. While the range of σ_n used for the interface envelopes is different, the interfaces with no hydration show a higher τ_p than the other interfaces. The interfaces with times of hydration of 24 and 48 hrs show essentially the same τ_p envelopes. The results in Fig. 5(b) indicate that, while interfaces will continue to hydrate beyond $t_h=24$ hrs, little further decrease in shear strength is expected to occur. A similar effect of t_h was noted for nonwoven GCL-GM interfaces (see FE 46, 47, 50).

The effect of σ_h on the peak shear strength of GCL A specimens hydrated during 24 hrs then sheared internally is shown in
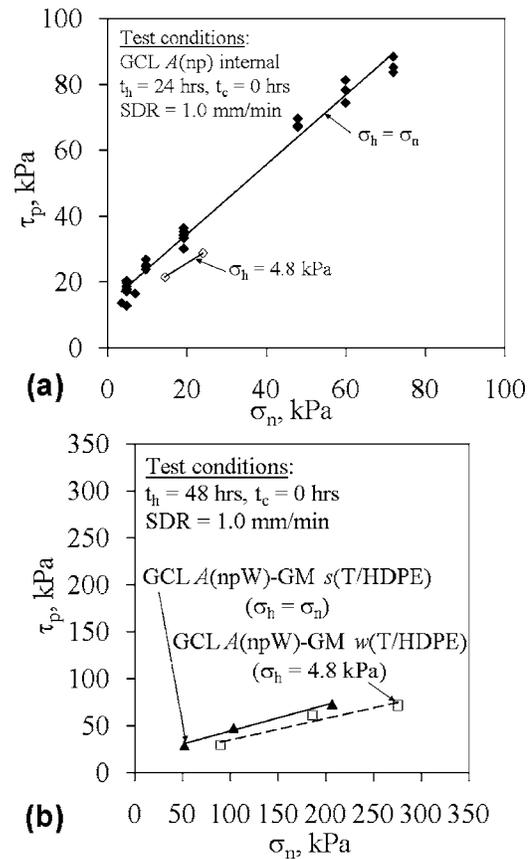
Fig. 6(a). The normal stress used for first failure envelope during hydration was $\sigma_h=\sigma_n$, while a constant, relatively low σ_h (4.8 kPa) was used in the other failure envelope. The normal stress in the latter failure envelope was increased from σ_h to σ_n without allowing consolidation of the bentonite before shearing ($t_c=0$ hrs). Despite some scatter in the data, the τ_p obtained when $\sigma_h=\sigma_n$ is consistently higher than that obtained when hydration is conducted using a relatively low σ_h. The effect of σ_h on the peak shear strength of woven GCL A-GM s interfaces hydrated during 48 hrs is shown in Fig. 6(b). The normal stress used for first failure envelope during hydration was $\sigma_h=\sigma_n$, while a constant, relatively low σ_h (4.8 kPa) was used in the other failure envelope. Similar to the GCL internal results, the τ_p obtained for the GCLs hydrated under $\sigma_h=\sigma_n$ is consistently higher than that obtained for the GCL-GM interfaces hydrated under a relatively low σ_h. Nonwoven GCL-GM interfaces were not sensitive to the hydration normal stress (see FE 47 and 48).
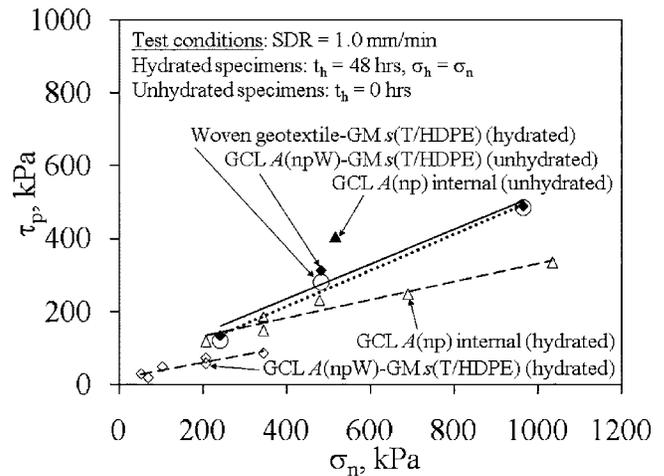
When GCLs are hydrated under a σ_h that is below σ_n, testing procedures often specify that the GCL be subsequently consolidated under the normal stress to be used during shearing. The effect of σ_h on τ_p and τ_{ld} for needle-punched GCL A specimens hydrated during 60 and 24 hrs then sheared internally is shown in Fig. 7(a). This figure includes data for GCL that were hydrated under $\sigma_h=\sigma_n$ (not consolidated) and subsequently sheared, and GCLs for which a constant, relatively low σ_h (6.9 kPa) was used. For the GCLs in which $\sigma_h<\sigma_n$, the normal stress was increased after hydration from σ_h to σ_n and 24 hrs was permitted for consolidation before shearing. While McCartney et al. (2004a) re-
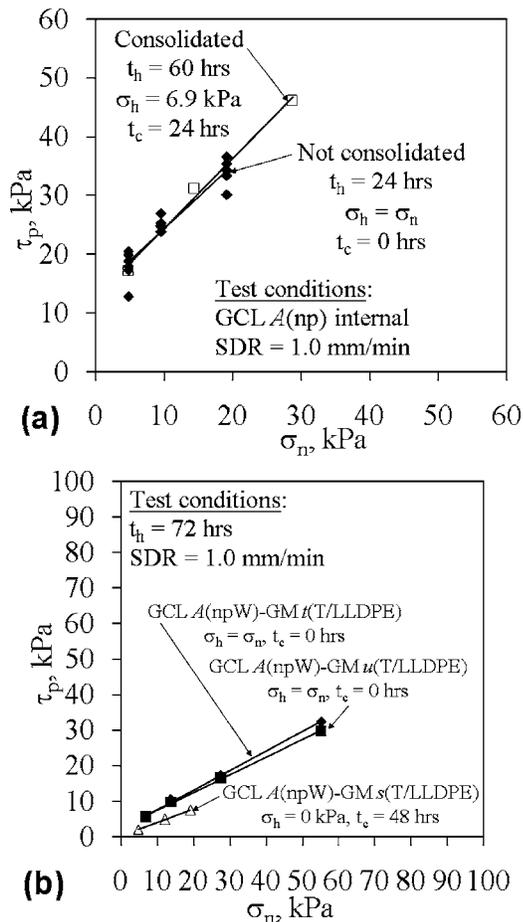
Fig. 7. Effect of consolidation when $\sigma_h < \sigma_n$ with $t_c > 0$ hrs on: (a) internal GCL peak shear strength; (b) woven GCL-GM interface peak shear strength

Fig. 8. Comparison of peak shear strength values from wetted geotextile-textured GM interface shear tests with those from GCL internal and GCL-textured GM interface shear tests using hydrated and unhydrated GCLs

ported that consolidation of GCLs led to a lower shear strength than specimens hydrated under $\sigma_h = \sigma_n$, reinterpretation of the data as shown in Fig. 7(a) indicates that the τ_p envelope obtained using $\sigma_h = \sigma_n$ is essentially the same as that obtained when the specimen is consolidated under σ_n after hydration using a relatively low σ_h. This observation contradicts results presented by other studies (Eid and Stark 1997; McCartney et al. 2004a). The effect of σ_h on the peak shear strength of the interface between the woven carrier geotextile side of GCL A and textured HDPE GMs is shown in Fig. 7(b). This figure includes results from tests on GCL-GM interfaces that were hydrated for 72 hrs under $\sigma_h = \sigma_n$ (not consolidated), and from tests on GCL-GM interfaces that were hydrated for 72 hrs under $\sigma_h = 0$ and consolidated under σ_n for 48 hrs. The shear strength of the GCL-GM interfaces that were hydrated using $\sigma_h < \sigma_n$ have lower shear strength after consolidation. This is inconsistent with the observations from GCL internal test results shown in Fig. 7(a). This investigation was also performed for nonwoven GCL-GM interfaces. While it appears that similar observations can be made from GCL-GM interfaces (see FE 47 and 52), the database did not include sufficient tests to evaluate the sensitivity of the peak shear strength of nonwoven GCL-GM interfaces to consolidation.

To better understand the role of GCLs in GCL-GM interface shear strength, the peak shear strength values obtained from GCL internal and GCL-GM interface shear tests with different hydration conditions are shown in Fig. 8, along with those from woven geotextile-GM interface shear tests. The interface tests include the same textured HDPE GM s and GCL A, and were sheared under both unhydrated and hydrated conditions. As expected, the highest τ_p was obtained for the unhydrated GCL sheared internally, due to the fiber reinforcements. The τ_p values from the wetted geotextile-GM interface and the unhydrated GCL-GM interfaces were slightly lower than the unhydrated GCL sheared internally, but were very similar. The τ_p values from the hydrated GCL sheared internally were found to not only be lower than that for the unhydrated GCL sheared internally, but also lower than those for the unhydrated GCL-GM interface. The lowest τ_p values were obtained for the hydrated GCL-GM interface. If the GCL did not play a role in the GCL-GM interface shear strength, the τ_p for the hydrated GCL-GM interface and the wetted geotextile-GM interface should have been similar. As this is not the case, it may be concluded that extrusion of bentonite from the GCL affected the shear behavior of the woven carrier geotextile side of the GCL-GM interface.

The observations from Fig. 8 allow interpretation of the similarity between the trends in GCL internal and GCL-GM interface shear strength with hydration (Figs. 5 and 6), and the lack of similarity between the trends in GCL internal and GCL-GM interface shear strength with consolidation (Fig. 7). The decrease in GCL-GM interface shear strength with t_h and σ_h observed in Figs. 5(a) and 6(b) occur because of extrusion of sodium bentonite from the GCL during hydration. Extruded bentonite: (i) lubricates connections between needle-punched fibers and the GM asperities; and (ii) acts as a plane of weakness with shear strength less than that of an internally reinforced GCL and a GM-geotextile interface (Gilbert et al. 1997; Triplett and Fox 2001). Further, subsequent consolidation of the GCL-GM interface was found from analysis of the data in Fig. 7(b) not to result in an increase in shear strength due to the weakening of the GCL-GM interface with bentonite extruded from the GCL during hydration and consolidation. If σ_h is below the swelling pressure of the bentonite (100 to 200 kPa), bentonite extrusion is expected to occur during hydration. If higher σ_h is used, extrusion is less likely. The volume of extruded bentonite is expected to increase with hydration time and probably also depends on the normal stress used during hydration (σ_h). Further, if a GCL-GM interface is consolidated
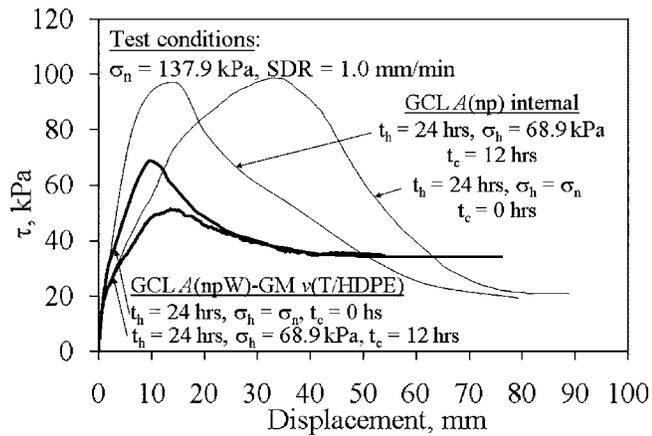
Fig. 9. Comparison between GCL-GM interface shear stress-displacement curves for different conditioning procedures

after having been hydrated under a low σ_h, additional extrusion is expected during consolidation due to the high hydraulic gradients caused by the increase in load.

A comparison between GCL internal and woven GCL-textured GM interface shear stress-displacement curves is shown in Fig. 9, for tests involving hydration under $\sigma_n = 68.9$ kPa followed by consolidation for 12 hrs under $\sigma_n = 137.9$ kPa before shearing. In addition, GCL internal and woven GCL-textured GM interface shear stress-displacement curves are presented for tests involving hydration and shearing under $\sigma_h = \sigma_n = 137.9$ kPa. Consistent with the results observed in Fig. 1, the internal and interface curves have a similar initial response for comparatively small shear displacements. This suggests that shearing develops initially within the GCL but shearing subsequently develops along the GCL-GM interface. Further, the shear displacement curve for the unconsolidated GCL-GM interface matches the curve for the consolidated GCL-GM interface (as well as the GCL internal curve) at small displacements. However, the curve for the unconsolidated GCL-GM interface shows a steep increase to a peak value of 69 kPa while that for the consolidated GCL-GM interface shows a more gradual increase to a peak value of 51 kPa. The curves for both GCL-GM interfaces show similar shear stress at larger shear displacements (beyond 25 mm). The difference in shear displacement response with conditioning procedures suggests that more bentonite extrusion, and a corresponding decrease in shear stress, occurred along the consolidated GCL-GM interface before shearing. However, all of the interfaces had similar GCL-GM interface large-displacement shear strength likely equal to the shear strength of the extruded bentonite. Although not a general trend, the GCLs sheared internally show higher peak shear strength (99 kPa) yet their large-displacement shear strength (20 kPa) is lower than that of the GCL-GM interfaces (34 kPa).

Variability

An evaluation of the variability in GCL internal shear strength is provided by Zornberg et al. (2005). The number of interface shear strength test results in the GCLSS database is large enough for assessment of GCL-GM interface shear strength variability. The different sources of interface shear strength variability can be quantified for use in reliability-based limit equilibrium analyses (McCartney et al. 2004a, b). Potential sources of variability in GCL-GM interface shear strength include: (i) differences in ma-

terial types (GCL reinforcement, carrier geotextile type, GM polymer, GM surface texturing); (ii) variation in test results from the same laboratory (repeatability); and (iii) overall material variability. In turn, the overall material variability includes more specific sources such as: (iii-a) inherent variability of fiber reinforcement and their interaction on the GCL surface with GM textured asperities; and (iii-b) inherent variability in the volume of extruded bentonite. Source of variability (i) is not addressed in this study since only the variability of individual GCL-GM interfaces is evaluated. The potential sources of variabilities (ii) and (iii) are assessed in this study using data presented in Table 5. This table presents nine sets of tests conducted using the same GCL and GM types, conditioning procedures, and σ_n.

Repeatability of Test Results Obtained from the Same Laboratory

The source of variability (ii) can be assessed by evaluating Sets V1, V2, and V3 in Table 5, which includes the results of tests conducted by a single laboratory using specimens collected from a single GCL and GM manufacturing lot, tested using the same conditioning procedures and same σ_n. For each set, Table 5 indicates the mean τ_p and τ_{ld} [$E(\tau_p)$ and $E(\tau_{ld})$], their standard deviations [$s(\tau_p)$ and $s(\tau_{ld})$], their COV values [$s(\tau)/E(\tau)$], and the maximum relative difference. Shear stress-displacement curves for woven GCL A-textured HDPE GM u interfaces are shown in Fig. 10 for interfaces with GM and GCL specimens from the same manufacturing lots, tested by the same laboratory, and using the same σ_n. These results illustrate that a very good repeatability can be achieved in the stress-displacement-strength response when tests are conducted by the same laboratory using same-lot specimens. The maximum relative difference in GCL-GM interface τ_p for specimens from the same manufacturing lots is less than 10%, which is well below the relative difference associated with different-lot specimens discussed next.

### Overall Material Variability

The source of variability (iii) may be assessed by evaluating Sets V4–V9 in Table 5. Unlike the results for Sets V1–V3 (Fig. 10), the GCL and GM specimens in Sets V4–V9 were obtained from different manufacturing lots. Each set of tests was conducted using the same GCL type, same GM (type, manufacturer, thickness), same conditioning procedures, and same σ_n. The maximum relative differences for Sets V4–V9 (approximately 50%) are significantly higher than those obtained for tests using GCL and GM specimens from rolls of the same lot (10%). Sets V4, V5, and V6 include data from 162 GCL-GM interface shear strength tests on GCL A and GM s conducted using the same conditioning procedures ($t_h = 168$ hrs, $t_c = 48$ hrs, SDR $= 0.1$ mm/min) and three different normal stresses ($\sigma_n = 34.5, 137.9, 310.3$ kPa). Subsets V4a to V4e, V5a to V5e, and V6a to V6e in Table 5 include the data from Sets V4, V5, and V6, respectively, grouped by the corresponding manufacturing year. Evaluation of statistical information on τ_p for V4–V6 shows an increasing $s(\tau_p)$ and a relatively constant COV with increasing σ_n, which indicates that τ_p variability increases linearly with σ_n. Fig. 11(a) shows the τ_p envelope obtained using the mean values of the 162 direct shear test results (Sets V4, V5, and V6 in Table 5). Significant scatter is noted in the results for tests conducted using the same GCL and GM types and conditioning procedures, but using specimens from different lots. The scatter likely arises due to differences in the surface roughness of the GCLs (reflected in variations in the

Table 5. GCL-GM Interface Data Sets for Assessment of Interface Shear Strength Variability

GCL-GM data set	GCL descrip.	GM Description	Thick-ness (mils)	t_h (hrs)	t_c (hrs)	SDR (mm/min)	σ_a (kPa)	Year GCL manufac.	Num. of tests	Peak strength[a] $E(\tau_p)$ (kPa)	$s(\tau_p)$ (kPa)	COV	Max. rel. diff. (%)	Large-displacement strength[a] $E(\tau_{ld})$ (kPa)	$s(\tau_{ld})$ (kPa)	COV	Max. rel. diff. (%)
V1	A(npW)	u(T/HPDE)	60	24	0	0.2	9.6	1996	2	5.8	0.4	N/A	9	4.9	0.1	N/A	4
V2	A(npW)	u(T/HPDE)	60	24	0	0.2	47.9	1996	2	18.1	0.4	N/A	3	12.9	0.0	N/A	0
V3	A(npW)	u(T/HPDE)	60	24	0	0.2	95.8	1996	2	37.0	0.4	N/A	2	27.0	0.4	N/A	2
V4	A(npW)	s(T/HPDE)	80	168	48	0.1	34.5	1997–2003	54	17.7	3.5	0.20	58	12.1	2.32	0.19	59
V4a	A(npW)	s(T/HPDE)	80	168	48	0.1	34.5	1997	3	20.5	3.2	0.16	23	13.1	1.38	0.11	19
V4b	A(npW)	s(T/HPDE)	80	168	48	0.1	34.5	1998	8	22.2	5.5	0.25	48	14.6	2.34	0.16	39
V4c	A(npW)	s(T/HPDE)	80	168	48	0.1	34.5	1999	9	18.1	1.8	0.10	28	11.9	1.61	0.14	30
V4d	A(npW)	s(T/HPDE)	80	168	48	0.1	34.5	2002	21	16.1	2.2	0.14	37	11.6	2.45	0.21	49
V4e	A(npW)	s(T/HPDE)	80	168	48	0.1	34.5	2003	13	16.8	2.1	0.13	33	11.5	1.82	0.16	38
V5	A(npW)	s(T/HPDE)	80	168	48	0.1	137.9	1997–2003	54	59.7	8.9	0.15	50	37.9	5.30	0.14	47
V5a	A(npW)	s(T/HPDE)	80	168	48	0.1	137.9	1997	3	53.1	6.9	0.13	23	31.5	6.22	0.20	33
V5b	A(npW)	s(T/HPDE)	80	168	48	0.1	137.9	1998	8	65.9	14.6	0.22	45	36.9	7.00	0.19	40
V5c	A(npW)	s(T/HPDE)	80	168	48	0.1	137.9	1999	9	57.0	11.3	0.20	45	33.6	5.88	0.18	43
V5d	A(npW)	s(T/HPDE)	80	168	48	0.1	137.9	2002	21	61.5	5.0	0.08	31	40.9	3.20	0.08	25
V5e	A(npW)	s(T/HPDE)	80	168	48	0.1	137.9	2003	13	56.1	5.2	0.09	24	38.1	2.82	0.07	22
V6	A(npW)	s(T/HPDE)	80	168	48	0.1	310.3	1997–2003	54	121.5	15.4	0.13	42	74.9	8.55	0.11	39
V6a	A(npW)	s(T/HPDE)	80	168	48	0.1	310.3	1997	3	117.2	15.5	0.13	23	61.6	2.22	0.04	6
V6b	A(npW)	s(T/HPDE)	80	168	48	0.1	310.3	1998	8	138.2	17.3	0.13	29	80.2	10.17	0.13	33
V6c	A(npW)	s(T/HPDE)	80	168	48	0.1	310.3	1999	9	114.3	18.6	0.16	36	71.2	6.88	0.10	28
V6d	A(npW)	s(T/HPDE)	80	168	48	0.1	310.3	2002	21	121.5	12.3	0.10	35	73.5	7.0S	0.10	31
V6e	A(npW)	s(T/HPDE)	80	168	48	0.1	310.3	2003	13	117.2	10.0	0.09	20	79.4	7.00	0.09	24
V7	A(npW)	s(T/HPDE)	80	24	0	1.0	172.4	1999	7	73.5	8.1	0.11	27	43.8	7.9	0.18	40
V8	A(npW)	s(T/HPDE)	80	24	0	1.0	344.7	1999	1	138.5	16.5	0.12	31	75.1	5.6	0.07	30
V9	A(npW)	s(T/HPDE)	80	24	0	1.0	689.5	1999	7	264.6	31.8	0.12	34	139.9	6.8	0.05	31

[a]$E(\tau)$=mean of τ, $s(\tau)$=standard deviation of COV=coefficient of variation of τ, maximum relative difference=$|\max(\tau)-\min(\tau)|/\max(\tau) \times 100\%$.

needle-punching process), the surface roughness of the GMs (reflected in variations in the asperity height), and the amount of bentonite extrusion during hydration and consolidation. The scatter in this figure has important implications on the selection of shear strength parameters for use in the design of slopes. McCartney et al. (2004b) summarizes the implications of project-specific and product-specific testing on relationships between the factor of safety and the probability of failure for infinite slopes.
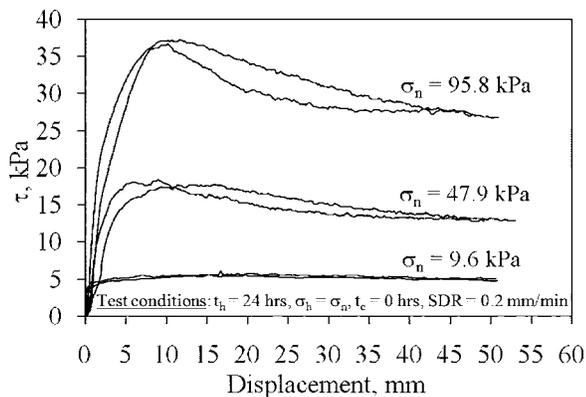

Fig. 10. Shear stress-displacement curves for GCL A(npW)-GM u(T/HDPE) interfaces with GCL and GM specimens obtained from the same manufacturing lots

Fig. 11(b) shows idealized normal probability density distributions for τ_p at each σ_n obtained using the same mean and standard deviation as the shear strength data for Sets V4, V5, and V6 in Table 5. These probability distributions quantify the statistical information on τ_p, which is useful for reliability-based design. Table 5 also includes statistical information regarding τ_{ld}. Although τ_{ld} may not be fully representative of the residual shear strength, the high COV of τ_{ld} indicates that GCL-GM interface large-displacement shear strength cannot be treated as a deterministic value.

Although comparisons between GCL internal and GCL-GM interface direct shear test results made in this study indicate that the average peak GCL internal shear strength is higher than the average peak GCL-GM interface shear strength, this observation should not be generalized. The ranges of GCL internal shear strength reported by Zornberg et al. (2005) are shown in Fig. 11(a). These data show that although the maximum GCL internal shear strength is significantly higher than the maximum GCL-GM interface shear strength, the minimum GCL internal shear strength is approximately the same as the average GCL-GM interface shear strength. This may have wide reaching impacts on the design of slopes incorporating a GCL and a GM. Further, as illustrated by the shear stress-displacement curves shown in Fig. 1, the large-displacement GCL-GM interface shear strength is often similar to that of GCLs sheared internally.

The 162 GCL specimens in Sets V4–V6 were received between Jan. 1997 and May 2003. In each subset, the COV and
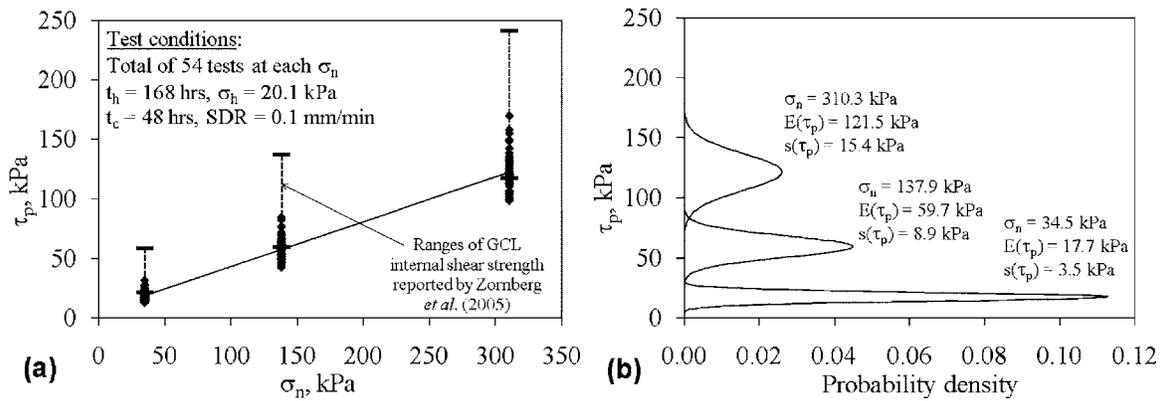
Fig. 11. Variability of the GCL A(npW)-GM s(T/HDPE) interface peak shear strength: (a) τ_p envelope; (b) normal probability distributions for τ_p at each σ_n

maximum relative difference is generally lower than for the overall multiyear data sets. The results in Table 5 indicate that the mean and the standard deviation values of the peak shear strength under the same normal stress are practically the same for the various GCL manufacturing years. The slight differences observed in variability from year to year are likely due to improvements in texturing of the GMs produced over time.

Sets V7–V9 in Table 5 include variability data from a set of 21 direct shear tests conducted using the same GCL tested in Sets V4, V5 and V6 (GCL A), but a different GM (GM v) and different conditioning procedures (t_h=24 hrs, t_c=0 hrs, SDR =1.0 mm/min). Three different σ_n (172.4, 344.7, and 689.5 kPa) were used in this program. The different GM and conditioning procedures led to a maximum relative difference in τ_p of approximately 30%. This maximum relative difference is smaller than that obtained for Sets V4, V5, and V6 using different conditioning procedures (~30%), suggesting that conditioning procedures may have some effect on the variability of interface GCL-GM test results.

Conclusions

A database of 534 GCL-GM interface shear strength tests was analyzed in this study. The data were obtained from large-scale (305 by 305 mm) direct shear tests conducted by a single laboratory over a period of 12 years using procedures consistent with current testing standards. Shear strength parameters were obtained to evaluate the effect of GCL and GM type, compare the shear strength of woven and nonwoven GCL interfaces, compare GCL internal and GCL-GM shear strength, evaluate the effect of GCL conditioning, and assess sources of GCL-GM interface shear strength variability. The following conclusions are drawn from this study:

1. The GCL-GM interface peak and large displacement shear strength values were found to be generally lower than the GCL internal peak and large-displacement shear strengths tested under normal stresses between 2.5 and 1,000 kPa, although both showed significant variability. However, comparison of the variability of GCL internal peak shear strength and the GCL-GM interface peak shear strength indicates that the GCL internal shear strength may potentially be lower than the GCL-GM interface shear strength if products from different manufacturing lots are used on a project. The large-displacement GCL-GM interface shear strength was often

found to be similar to that of GCLs sheared internally.

2. Analysis of the GCL-GM interface shear strength data indicates that the peak shear strength of nonwoven GCL-textured GM interface is higher than that of woven GCL-textured GM interface (for normal stresses between 2.4 and 1,000 kPa), and higher than that of woven GCL-smooth GM interfaces and nonwoven GCL-smooth GM interfaces. GCL internal shear strength envelopes are higher than those for woven and nonwoven GCL-GM interfaces, but have a similar friction angle.

3. The woven and nonwoven GCL-textured HDPE GM interface shear strengths are sensitive to the GCL type. Specifically, the woven needle-punched GCL interfaces were found to have higher interface shear strength than woven thermal-locked and stitch-bonded GCL interfaces.

4. Textured GM interfaces showed large postpeak shear strength loss, while smooth GM interfaces experienced essentially no postpeak shear strength loss.

5. The woven and nonwoven GCL-textured GM interface shear strengths were found to be sensitive to the GM flexibility for the set of interfaces tested in this study under normal stresses less than 50 kPa. Specifically, flexible GMs (e.g., VLDPE GMs) were found to have higher interface shear strength than stiffer GMs (e.g., HDPE GMs). The GCL-textured GM interfaces shear strengths were found not to be sensitive to the GM manufacturer or GM thickness.

6. Unlike results for GCLs sheared internally, the peak shear strength envelopes for woven and nonwoven GCL-GM interfaces showed a comparatively small cohesion intercept and remained linear for a wide range of σ_n. Similar large-displacement shear strength envelopes were found for GCL internal and woven and nonwoven GCL-GM interfaces.

7. Hydration was found to lead to a decrease in both GCL internal peak shear strength and woven GCL-GM interface peak shear strength. Hydration using a normal stress less than that used during shearing without allowing time for subsequent consolidation was found to lead to further decrease in GCL internal and woven GCL-GM interface peak shear strength. Subsequent consolidation of GCLs hydrated under a normal stress less than that used during shearing was found to lead to an increase in GCL internal shear strength, but a decrease in woven GCL-GM interface shear strength. Hydration and consolidation had a negligible effect on the peak shear strength of nonwoven GCL-GM interfaces.

8. The inconsistencies in the trends in GCL internal and woven

GCL-GM interface shear strength with hydration and consolidation were proposed to be due to bentonite extrusion. Hydrated GCL-GM interfaces were found to have lower peak shear strength than wetted geotextile-GM interfaces, indicating that the bentonite extrusion from the GCL plays an important role in the GCL-GM interface shear behavior. Interfaces involving nonwoven GCLs were found to be less affected by bentonite extrusion than interfaces involving woven GCLs.

9. Good repeatability was obtained for duplicate tests on GCLs and GMs from the same manufacturing lots (maximum relative difference of 10%). However, significant variability was obtained for GCL-textured GM interface with materials from different lots (maximum relative difference of 50%). The variability of GCL-GM interface shear strength was less than that for GCL internal shear strength, and normal stress, interface conditioning, GM manufacturer were found to impact the peak shear strength variability.

Acknowledgments

References

American Society of Testing and Materials. (2004). "Standard test method for determining average bonding peel strength between the top and bottom layers of needle-punched geosynthetic clay liners." *ASTM D6496*, West Conshohocken, Pa.

American Society of Testing and Materials. (2008). "Standard test method for determining the internal and interface shear resistance of geosynthetic clay liner by the direct shear method." *ASTM D6243*, West Conshohocken, Pa.

Chiu, P., and Fox, P. J. (2004). "Internal and interface shear strengths of unreinforced and needle-punched geosynthetic clay liners." *Geosynthet. Int.*, 11(3), 176–199.

Eid, H. T., and Stark, T. D. (1997). "Shear behavior of an unreinforced geosynthetic clay liner." *Geosynthet. Int.*, 4(6), 645–659.

Fox, P. J., and Stark, T. (2004). "State of the art report: GCL shear strength and its measurement." *Geosynthetics Int.*

Gilbert, R. B., Fernandez, F. F., and Horsfield, D. (1996). "Shear strength of a reinforced clay liner." *J. Geotech. Geoenviron. Eng.*, 122(4), 259–266.

Gilbert, R. B., Scranton, H. B., and Daniel, D. E. (1997). "Shear strength testing for geosynthetic clay liners." *Testing and acceptance criteria for geosynthetic clay liners*, L. Well, ed., American Society for Testing and Materials, Philadelphia, 121–138.

Hewitt, R. D., Soydemir, C., Stulgis, R. P., and Coombs, M. T. (1997). "Effect of normal stress during hydration and shear on the shear strength of GCL/textured geomembrane interfaces." *Testing and acceptance criteria for geosynthetic clay liners*, L. Well, ed., American Society for Testing and Materials, Philadelphia, 55–71.

Ivy, N. (2003). "Asperity height variability and effects." *GFR. Oct.*, 28–29.

Lake, C. G., and Rowe, R. K. (2000). "Swelling characteristics of needle-punched, thermal treated geosynthetic clay liners." *Geotext. Geomembr.*, 18, 77–101.

McCartney, J. S., Zornberg, J. G., and Swan, R. H., Jr. (2004a). "Effect of specimen conditioning on gcl shear strength." *Proc. Geoasia 2004: 3rd Asian Regional Conf. on Geosynthetics*, J. G. Shim, C. Yoo, and H.-Y. Jeon, eds., Korean Geosynthetics Society, Seoul, Korea, 631–643.

McCartney, J. S., Zornberg, J. G., and Swan, R. H., Jr. (2005). "Effect of geomembrane texturing on geosynthetic clay liner—Geomembrane interface shear strength." *Proc., GeoFrontiers 2005* (CD-ROM), ASCE.

McCartney, J. S., Zornberg, J. G., Swan, R. H., Jr., and Gilbert, R. B. (2004b). "Reliability-based stability analysis considering GCL shear strength variability." *Geosynthet. Int.*, 11(3), 212–232.

Triplett, E. J., and Fox, P. J. (2001). "Shear strength of HDPE geomembrane/geosynthetic clay liner interfaces." *J. Geotech. Geoenviron. Eng.*, 127(6), 543–552.

Zornberg, J. G., and McCartney, J. S., Swan, R. H. (2005). "Internal shear strength of geosynthetic clay liners." *J. Geotech. Geoenviron. Eng.*, 131(3), 1–14.